

# Feature guided waves (FGW) in fiber reinforced composite plates with 90° transverse bends

Cite as: AIP Conference Proceedings **1706**, 030016 (2016); <https://doi.org/10.1063/1.4940488>  
Published Online: 10 February 2016

Xudong Yu, Madis Ratassepp, Zheng Fan, Prabhakaran Manogharan, and Prabhu Rajagopal



View Online



Export Citation

## ARTICLES YOU MAY BE INTERESTED IN

[Feature-guided waves \(FGW\) in plate structures with 90° transverse bends](#)

AIP Conference Proceedings **1650**, 713 (2015); <https://doi.org/10.1063/1.4914672>

[Interaction of guided waves with delaminations in composite plate structures](#)

AIP Conference Proceedings **1806**, 030011 (2017); <https://doi.org/10.1063/1.4974579>

[A two-dimensional Fourier transform method for the measurement of propagating multimode signals](#)

The Journal of the Acoustical Society of America **89**, 1159 (1991); <https://doi.org/10.1121/1.400530>

Lock-in Amplifiers  
up to 600 MHz



# Feature Guided Waves (FGW) in Fiber Reinforced Composite Plates with 90° Transverse Bends

Xudong Yu<sup>1</sup>, Madis Ratssepp<sup>1</sup>, Zheng Fan<sup>1,a)</sup>, Prabhakaran Manogharan<sup>2</sup> and Prabhu Rajagopal<sup>2</sup>

<sup>1</sup>*School of Mechanical and Aerospace Engineering, Nanyang Technological University, 50 Nanyang Avenue, Singapore 639798.*

<sup>2</sup>*Centre for Nondestructive Evaluation and Department of Mechanical Engineering, Indian Institute of Technology Madras, Chennai-600036, Tamil Nadu, India.*

<sup>a)</sup>Corresponding author: ZFAN@ntu.edu.sg

**Abstract.** Fiber reinforced composite materials have been increasingly used in high performance structures such as aircraft and large wind turbine blades. 90° composite bends are common in reinforcing structural elements, which are prone to defects such as delamination, crack, fatigue, etc. Current techniques are based on local inspection which makes the whole bend area scanning time consuming and tedious. This paper explores the feasibility of using feature guided waves (FGW) for rapid screening of 90° composite laminated bends. In this study, the behavior of the bend-guided wave in the anisotropic composite material is investigated through modal studies by applying the Semi-Analytical Finite Element (SAFE) method, also 3D Finite Element (FE) simulations are performed to visualize the results and to obtain cross validation. To understand the influence of the anisotropy, three-dimensional dispersion surfaces of the guided modes in flat laminated plates are obtained, showing the dependence of the phase velocity with the frequency and the fiber orientation.  $SH_0$ -like and  $S_0$ -like bend-guided modes are identified with energy concentrated in the bend region, limiting energy radiation into adjacent plates and thus achieving increased inspection length. Finally, parametric studies are carried out to further investigate the properties of these two bend-guided modes, demonstrating the variation of the group velocity, the energy concentration, and the attenuation with the frequency.

## INTRODUCTION

Fiber reinforced composite materials become widely used as critical structural components for a significant amount of applications ranging from aerospace systems to automotive, industrial and consumer products. Because of their high strength to weight ratio, good stiffness properties, and inherent corrosion resistance, fiber reinforced composites are being developed to be attractive alternatives, replacing metal components in primary and secondary aircraft structures [1, 2, 3, 4]. This brings new challenges in the manufacturing of specific components as well as in the non-destructive testing (NDT) of the structure throughout its service life. For instance, 90° composite bends are common in reinforcing elements like spars and stiffeners, and due to the stress concentration the bend region is prone to defects such as delamination, crack, fiber waviness and fatigue, which can severely compromise the structural integrity. Current techniques to inspect these bends require scanning with ultrasonic probes such as phased arrays with selected wedges over the whole region of interest, which is time consuming and tedious. Moreover, specific wedges are needed for bends with different bend radius, and the wedges are worn out easily during testing.

In such context, this paper explores the feasibility of using feature guided waves (FGW), which the energy is concentrated in local features for rapid screening of 90° composite laminated bends. This idea comes from the authors' previous studies of the wave's feature guiding phenomena in 90° metallic bends, which suggest the presence of low dispersive and low attenuative bend-guided waves and their capability of focusing the energy in the bend [5, 6]. In this new study,  $SH_0$ -like and  $S_0$ -like bend-guided modes have been identified in the 90° unidirectional composite laminated bend. Both modes have little dispersion and low attenuation, with propagation energy strongly concentrated in the bend region, which are very attractive for the NDT of long-range composite bends.

This paper starts with an investigation on dispersion characteristics of the unidirectional composite plate. It is followed by a summary of modeling methods to identify and understand FGWs in composite bends. Modal studies of the bent plate are carried out using the SAFE method. 3D FE simulations are performed to obtain the wave field of propagating FGWs. Following that, parametric studies are conducted to study variation of properties of the FGWs with the frequency. Finally, the paper concludes modeling results and indicates the future work.

## DISPERSION CHARACTERISTICS OF COMPOSITE PLATES

Before proceeding to FGWs in composite bends, it is essential to understand the guided wave propagation in a flat unidirectional laminate. In this study, a graphite epoxy composite material T300/914 [7], which is considered to be elastic (undamped) and transversely isotropic, was used for demonstration. The mass density of such material is  $1560 \text{ kg/m}^3$  and its elastic constants are given in Table 1 in the principal directions of material symmetry, where  $x_1$  is the fiber direction,  $x_2$  is the direction perpendicular to the fibers in the laminate plane, and  $x_3$  is the through-thickness direction. The reference coordinates are shown in Fig. 1.

**TABLE 1.** Elastic constants (in GPa) for the T300/914 laminate examined in Ref. [8] and in the present study.

$C_{11}$	$C_{12}$	$C_{13}$	$C_{22}$	$C_{23}$	$C_{33}$	$C_{44}$	$C_{55}$	$C_{66}$
143.8	6.2	6.2	13.3	6.5	13.3	3.6	5.7	5.7

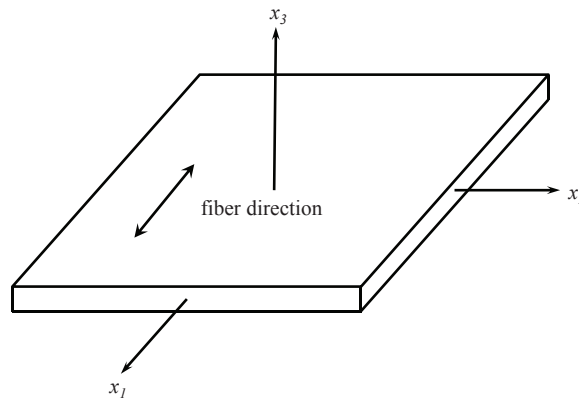


**FIGURE 1.** Reference coordinates of unidirectional fiber reinforced laminate.

Figure 2(a) shows the phase velocity dispersion curves for modes propagating along the fiber direction ( $0^\circ$ ), calculated by the methods based on the superposition of bulk waves (SPBW) [9]. Results obtained by the SPBW and the SAFE methods are in an exact agreement. For propagation in the principal directions, parallel and normal to the fiber direction, the vertically and horizontally polarized partial waves are de-coupled and behave similarly to the equivalent modes in isotropic materials. However, if the propagation is along the non-principal axis, it is no longer possible to trace the Lamb and the SH modes separately due to the coupling effect between them [10, 11]. Therefore wave propagation in such composite plates is angle dependent. To further illustrate this, three-dimensional dispersion surfaces of the  $S_0$  and the  $SH_0$  modes are plotted in Fig. 2 (b) and (c), with respect to the frequency and the wave propagation angle, which were derived by the SAFE method. It can be observed that not only the propagation velocity but also the dispersion nature of the modes is influenced by the fibers. The phase velocity of the  $S_0$  mode decreases with the propagation angle deviating from the fiber direction. The  $SH_0$  mode is non-dispersive in the  $0^\circ$  and  $90^\circ$  directions, but has different degrees of dispersion at other angles.

In recent aerospace structural applications, laminated composites are molded into complex shapes and one typical example is our studied case - the  $90^\circ$  transverse bend. On the basis of characteristics discussed above, this study starts with the exploration of FGWs propagating along fibers in composite laminated bends.

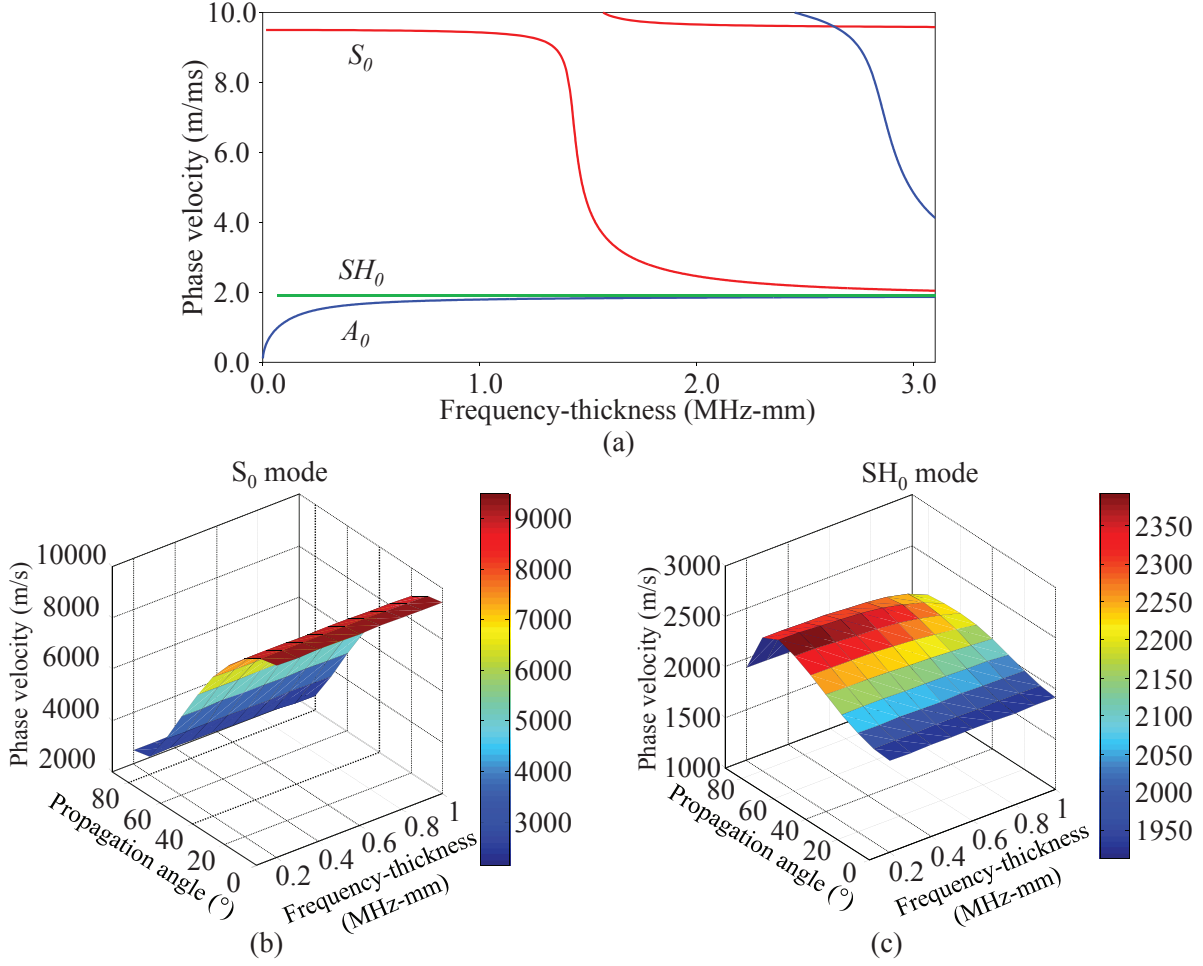


**FIGURE 2.** (Color online) Dispersion curves of unidirectional laminates: (a) wave propagation along the fiber direction ( $0^\circ$ ); (b) dispersion surface of the  $S_0$  mode; (c) dispersion surface of the  $SH_0$  mode.

## MODELING METHODS

FGWs here are the trapped modes propagating in the bend along the  $x_3$  direction shown in Fig. 3, which is also the fiber direction in this study.

### Semi-Analytical Finite Element (SAFE) Method

Modal studies for the bent plate with anisotropic properties were carried out by applying the well-known SAFE method [12]. It solves an eigenvalue problem of the solid with constant waveguides to find all possible propagation modes at a chosen frequency. The schematic of the model is shown in Fig. 3(a), in which the bend radius  $R_B$  is 4 mm and the thickness of the bent plate is 2 mm. Quadratic triangular elements were used to mesh the entire model with finer element size in the bend region than that in adjacent plates. Stress-free boundary conditions were applied to boundaries enclosing the plate. The same elastic properties as laminates studied in the last section were assigned to the cross section. In the SAFE model the propagation direction is always in the  $x_3$  direction (perpendicular to the cross section), therefore the stiffness matrix based on the coordinate system shown in Fig. 1 needs to be rotated according to [1]:

$$[C'] = [T][C][T]^t, \quad (1)$$

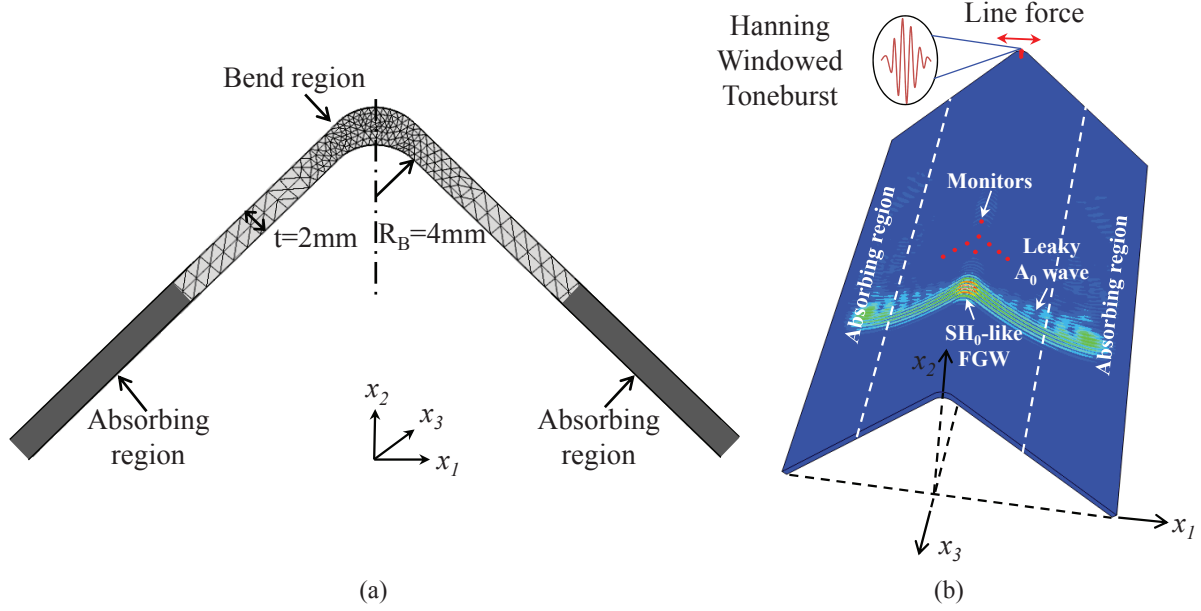


**FIGURE 3.** (Color online) Schematics of (a) the SAFE model and (b) 3D FE model of the bent plate.

where  $[C]$  is the stiffness matrix in the lamina's principal direction, and  $[T]$  is the rotation matrix. In addition, the plate sides were extended by absorbing region to avoid the interference by reflections from the edges.

### 3D Finite Element Simulation

In a separated model study, the wave propagation in the anisotropic bend was simulated using a 3D FE model in a commercial FE package [13], similarly as the work on the  $90^\circ$  metallic bend that the authors reported earlier [5]. A snapshot of the earlier work is shown in Fig. 3(b). The model was set up to represent the same geometry and elastic properties as that used in the SAFE model. The three-dimensional model was meshed by 8-node brick elements (C3D8R) and the element size is selected such that it has at least 12 elements per wavelength of bend-guided modes [14]. In the FE model, a local coordinate system is defined to assign material properties to each of the elements in the model.

The model was excited by applying a 5-cycle Hanning windowed tone burst force signals in the  $x_1$  or  $x_3$  direction along all nodes of a through-thickness nodal line at the plate end bisecting the bend region. The model was solved in the time domain at frequencies ranged from 100 kHz to 500 kHz. An iteration step time of  $5e-9$  seconds was used to adhere to the usual stability criterion [15, 16].

## RESULTS

### Identification of Bend-guided Modes

Potential feature guided wave modes can be identified from their axial components of the time-averaged power flow (along the bend direction), namely the Poynting vector [17]:

$$P_{x_3} = -\text{Re}\left[\left(\frac{I\omega}{2}\right)(u_1^* \sigma_{31} + u_2^* \sigma_{32} + u_3^* \sigma_{33})\right], I = \sqrt{-1}, \quad (2)$$

where  $\sigma_{31}$ ,  $\sigma_{32}$  and  $\sigma_{33}$  are components of the axial stress;  $u_1^*$ ,  $u_2^*$  and  $u_3^*$  denote the complex conjugate of the horizontal, vertical, and axial displacements of the modes, respectively. In the SAFE model, the bend-guided mode can be identified as its propagation energy is concentrated into the bend region. The purpose of this study is to find eigen-wavenumber solutions that represent guided wave modes propagating along the bend. Two bend-guided modes, namely the  $SH_0$ -like and the  $S_0$ -like bend-guided modes, were discovered in the anisotropic bend as shown by Fig. 4 and 5, respectively.

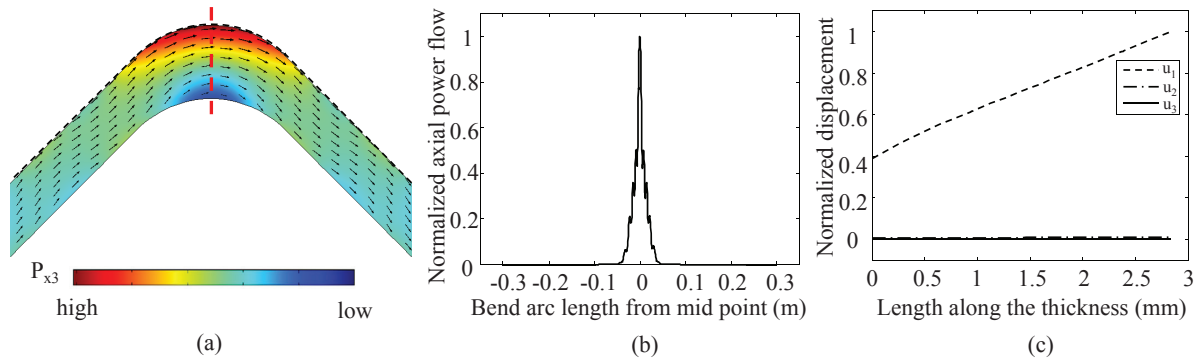


**FIGURE 4.** (Color online) (a) Axial power flow variation of the  $SH_0$ -like bend-guided mode in the cross section, derived from the SAFE model at 1 MHz; (b) normalized axial component of power flow along the outer boundary (dashed line, black) of the bent plate; (c) displacement mode shape extracted along through-thickness cutline (dashed line, red).

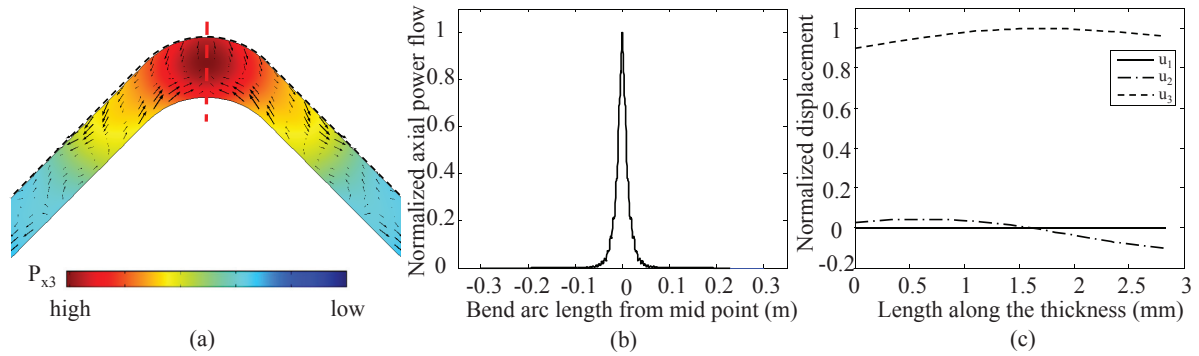


**FIGURE 5.** (Color online) (a) Axial power flow variation of the  $S_0$ -like bend-guided mode at 400 kHz; (b) normalized axial power flow of the bent plate; (c) through-thickness displacement mode shape.

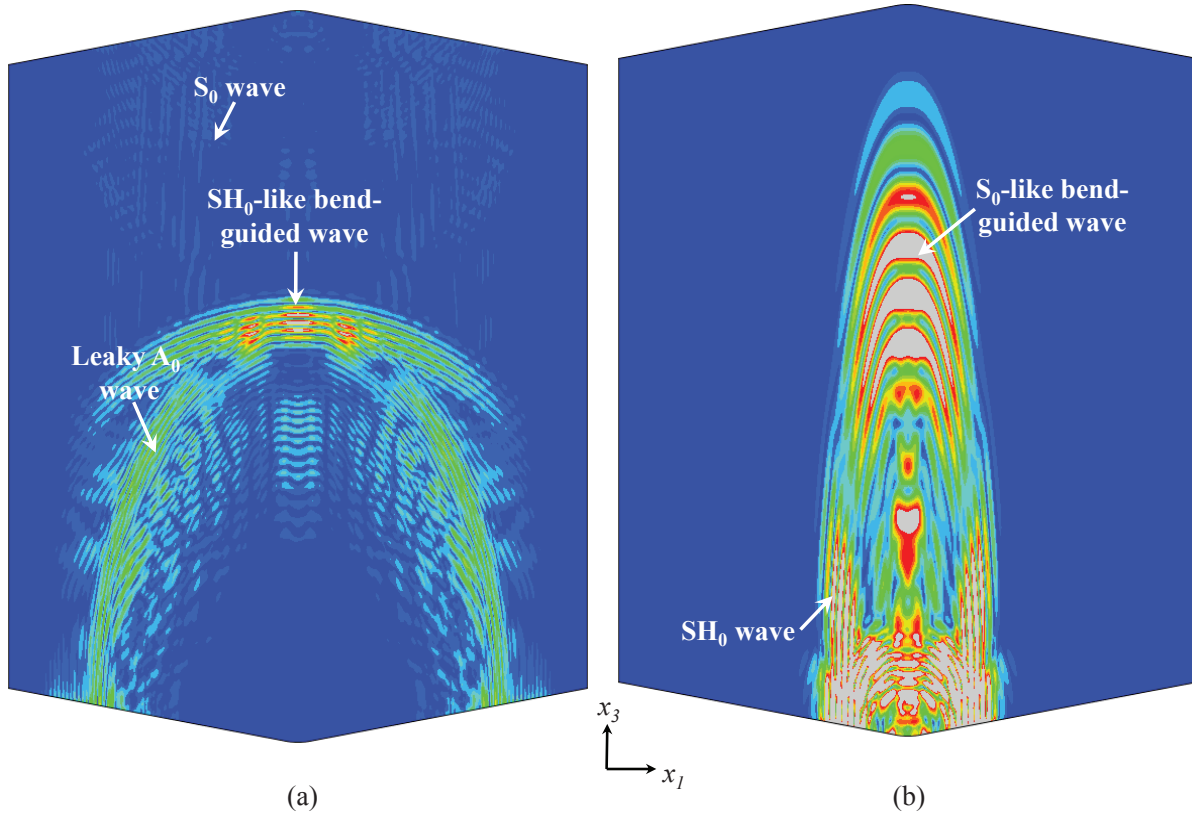
Figure 4(a) illustrates the axial power flow of the  $SH_0$ -like mode in the cross section at 1 MHz with color coding denoting its relative amplitudes, and Fig. 4(b) plots its quantity along the outer boundary of the bent plate. The amplitudes of the axial power flow were normalized by the peak value in the bend region. It can be seen that the identified  $SH_0$ -like bend-guided wave mode shows strong energy concentration in the bend region. Its mode shape shown in Fig. 4(c) is similar to the fundamental shear horizontal mode ( $SH_0$ ) propagating in unidirectional composite plate along the fiber direction, which is dominated by the in-plane displacement, but with variation through the thickness. The arrow shown in Fig. 4(a) represents the particle displacement in the cross section with its length proportional to the magnitude of the particle displacement.

Figure 5 depicts the power flow variation around the bend and extracted mode shape of the  $S_0$ -like bend-guided mode at 400 kHz. It can be observed that the  $S_0$ -like bend-guided mode retains significant energy in the bend as well. Its mode shape, similar to the compression mode ( $S_0$ ) in a laminated plate, is dominated by the axial displacement. And the axial component is almost constant through the thickness.

### Wave Field of Bend-guided Waves

In order to validate the existence of identified bend-guided modes, 3D FE simulations were carried out. In the FE models, amplitudes of the resultant displacement of the whole wave field were obtained as shown in Fig. 6. Forcing in the in the  $x_1$  or  $x_3$  direction was introduced at the plate bend to excite the bend-guided waves.

Figure 6(a) and (b) present instant snapshots of the propagation of the  $SH_0$ -like and the  $S_0$ -like bend-guided waves at the central frequency of 500 kHz and 400 kHz, respectively, with color contour showing magnitudes of the resultant displacement. It can be seen that in both cases the amplitude of displacement in the bend region is much higher than that in the adjacent plate, which indicates that the energy is highly focused in the bend and is guided along the fiber direction. We also noted that both modes propagate with limited radiation into adjacent plates.



**FIGURE 6.** (Color online) Snapshot of the wave propagation in the unidirectional composite bent plate: (a)  $SH_0$ -like bend-guided wave at 500 kHz excited by forcing in the  $x_1$  direction applied at the plate end; (b)  $S_0$ -like bend-guided wave at 400 kHz with excitation in  $x_3$  direction; color coding shows relative displacement amplitude of propagation modes (blue: low to red: high).

### Properties of Bend-guided Waves

To further investigate properties of the two bend-guided modes in composites, parametric studies were conducted by using the SAFE method to understand the dependence of the group velocity, the energy concentration, the attenuation with the frequency.

Group velocity dispersion curves for the two trapped modes are shown in Fig. 7(a). The group velocity of the bend-guided modes is calculated as  $c_{gr} = \partial\omega/\partial k'$  ( $k'$  is the real part of the complex eigen-wavenumber  $k$ ). It is worth noting that the energy velocity should be the exact solution of the velocity of the wave-packet, at which the wave carries its potential and kinetic energy along the structure [17, 18]. However, it is reasonably accurate if the attenuation is small and only the real part of the wavenumber is used for calculation. Using the 3D FE approach, displacement in  $x_1$  or  $x_3$  direction were monitored (see Fig. 3 for illustration of coordinate axes) at the top surface of the bend with several distances away from the source. It can be seen that the  $SH_0$ -like bend-guided mode is almost non-dispersive from 100 kHz to 500 kHz, while the  $S_0$ -like mode also has little dispersion at lower frequencies and becomes more dispersive at higher frequencies. The SAFE predictions are in close agreement with FE results.

The Full width at Half Maximum (FWHM) of the axial power flow curves shown in Fig. 4(b) and Fig. 5(b), is used to quantify their energy focusing in the feature (along the bend arc) [19]. The FWHM is measured as the width

of axial power flow between two points on the curve whose values are half of the maximum. The smaller the value of the FWHM is, the more the energy is concentrated in and around the bend. It can be observed from Fig. 7(b) that the FWHM of both modes decreases as the frequency increases, which indicates that more energy is concentrated in the bend at higher frequencies. The  $SH_0$ -like mode is capable of retaining energy firmly in the bend, while the  $S_0$ -like mode shows much variation of the energy concentration with the frequency.

The attenuation dispersion curve of the two modes is plotted in Fig. 7(c). It can be seen that the attenuation of the  $SH_0$ -like mode is low and decreases at higher frequencies. The  $S_0$ -like mode has even lower attenuation at lower frequencies. This suggests that both modes have little energy radiation to adjacent plates and the most energy is still trapped in the bend, which are therefore very promising for rapid screening of long composite bends.

In addition, as to the physics of energy trapping effect shown here, it can be explained by the well-known Snell-Descartes law [17]. This has been demonstrated in previous publications [19, 20] that for the feature guided mode to exist, two criteria have to be satisfied: the propagation mode in the local feature, which in our case is the bend region, should have similar mode shape to the corresponding mode in the adjacent plate and their phase velocities should be slower. This has been verified in both cases of the  $SH_0$ -like and the  $S_0$ -like bend-guided modes discussed here.

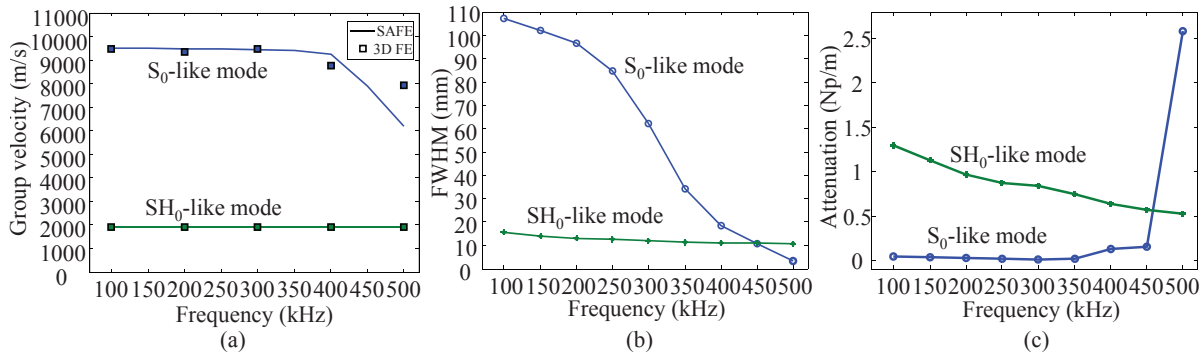


FIGURE 7. (a) Group velocity dispersion curves, derived by the SAFE method and 3D FE simulations; (b) spectrum of the FWHM from 100 kHz to 500kHz; (c) attenuation dispersion curves of bend-guided modes.

## DISCUSSION AND CONCLUSION

The  $SH_0$ -like and  $S_0$ -like bend-guided modes have been identified in the  $90^\circ$  unidirectional composite bend by applying the SAFE method, and their characteristics have been cross verified by 3D FE simulations. Both modes show strong energy confinement in the bend with low attenuation and little dispersion, thus they have great potential for quick inspection of delamination in long-range composite bends.

This study has validated the modeling methodology of FGWs in structural bends with anisotropic material properties. It lays the foundation for exploring FGWs in multidirectional composite bends, which are more common in the industry.

## ACKNOWLEDGMENTS

This work was supported by the Start Up Grant (SUG) from the Nanyang Technological University.

## REFERENCES

- 1 S. Rokhlin, D. Chimenti, and P. Nagy, *Physical ultrasonics of composites* (Oxford University Press, 2011).
- 2 I. M. Daniel and O. Ishai, *Engineering mechanics of composite materials* (Oxford university press, New York, 2006).
- 3 G. A. Matzkanin and H. T. Yolken, *AMMTIAC Quarterly* **2**, 3–7 (2007).

- 4 J. Eihusen, "Characterization of the transverse thermal conductivity of intraply hybrid composite laminates," in *31 st International SAMPE Technical Conference* (1999), pp. 211–220.
- 5 X. Yu, P. Manogharan, Z. Fan, and P. Rajagopal, "Feature-guided waves in plate structures with 90° transverse bends," in *Review of Progress in Quantitative Nondestructive Evaluation*, Vol. 34, edited by D. E. Chimenti and L. J. Bond (American Institute of Physics 1650, Melville, NY, 2015), pp. 713–720.
- 6 P. Manogharan, X. Yu, Z. Fan, and P. Rajagopal, *NDT & E International* **75**, 39–47 (2015).
- 7 S. C., K. H., and R. D., "Elastic wave propagation along arbitrary direction in free orthotropic plate. application of composite materials." in *4th French Congress on Acoustics* (1997).
- 8 B. N. Pavlakovic, M. J. S. Lowe, D. N. Alleyne, and P. Cawley, "Disperse: A general purpose program for creating dispersion curves," in *Review of Progress in Quantitative Nondestructive Evaluation*, Vol. 16, edited by D. O. Thompson and D. E. Chimenti (Plenum Press, New York, 1997), pp. 185–192.
- 9 M. J. S. Lowe, *IEEE Trans. Ultrason. Ferroelectr. Freq. Control* **42**, 525–542 (1995).
- 10 B. N. Pavlakovic and M. J. S. Lowe, Copyright B. Pavlakovic, M. Lowe (2003).
- 11 I. Bartoli, A. Marzani, F. L. Scalea, and E. Viola, *Journal of Sound and Vibration* **295**, 685–707 (2006).
- 12 M. V. Predoi, M. Castaings, B. Hosten, and C. Bacon, *J. Acoust. Soc. Am.* **121**, 1935–1944 (2007).
- 13 ABAQUS, *Abaqus Keywords Reference Guide* (Version 6.13 by Dassault Systèmes, <http://www.3ds.com/>, 2013).
- 14 D. N. Alleyne, B. Pavlakovic, M. J. S. Lowe, and P. Cawley, *Insight* **43**, 93–96,101 (2001).
- 15 E. Le Clézio, M. Valentin Predoi, M. Castaings, B. Hosten, and M. Rousseau, *Ultrasonics*. **41**, 25–40 (2003).
- 16 P. Rajagopal and M. J. S. Lowe, *J. Acoust. Soc. Am.* **124**, 2895–2904 (2008).
- 17 B. A. Auld, *Acoustic Fields and Waves in Solids*, Vol. 1 (Krieger Publishing Company, Malabar, Florida, 1990).
- 18 A. Bernard, M. J. S. Lowe, and M. Deschamps, *J. Acoust. Soc. Am.* **110**, 186–196 (2001).
- 19 Z. Fan and M. J. Lowe, *Proceedings of the Royal Society A: Mathematical, Physical and Engineering Science* **465**, 2053–2068 (2009).
- 20 A. Ramdhas, R. K. Pattanayak, K. Balasubramaniam, and P. Rajagopal, *J. Acoust. Soc. Am.* **134**, 1886–1898 (2013).